UCLouvain
Faculté des sciences

Centre for Cosmology, Particle Physics and Phenomenology

MadSpin Density :

A new approach to the computation of matrix elements

Author : Quentin Heirebaudt
Thesis Director : Fabio Maltoni
Readers : Christophe Delaere and Olivier Mattelaer
Academic Year 2022-2023

In order to obtain the Degree
Master [120] en sciences physiques, finalité approfondie

Ecole de Physique, Marc de Hemptinne
Chemin du Cyclotron 2, boîte L7.01.04,
1348, Louvain-la-Neuve

MadSpin Density : a new approach to the computation of matrix elements

Quentin Heirebaudt (38051700)

Master Thesis

Supervisor: F. Maltoni

Readers: C. Delaere and Olivier Mattelaer

Academic Year 2022- 2023

UCLouvain
École de physique

Contents

Acknowledgements

The content of this Master's thesis has been corrected and reviewed on a regular basis by Olivier Mattelaer. By guiding my work, questionning my methods and providing me with new insights and intuitions, he encouraged me to dig further and with more determination. Our Friday morning meetings enabled me to have regular and fruitful discussions about any subjects encountered. He systematically came forward whenever I had doubts or concerns and made me feel legitimate in the process. I am deeply grateful for his help I could always count on. I also thank Fabio Maltoni for agreeing to supervise this Master's thesis and for the time given to the reading of the next pages. Many thanks also to Christophe Delaere for being a reader of this thesis.

I want to thank my partner who has always supported me throughout the past years. By reviewing, correcting and giving me great insights, she has played a special part in the genesis of this work. I also thank my parents for their support throughout all of my years as a student. I feel Lucky to be well surrounded.

Abstract

In this Master's thesis, MadSpin density mode is introduced. This new method within the MadSpin framework aims at computing matrix elements using only the production and the decay parts of a diagram while keeping the spin correlation effects. This is done relying on the Narrow Width Approximation as well as on the MadGraph's capacity to compute production and decay matrix elements. The theoretical aspects are introduced and the method used for a few processes. Even tough the current implementation does not allow more than one decaying particle, MadSpin density should allow the computation of matrix elements for processes that were not allowed in MadSpin e.g. loop induced processes as well as interferences between the Standard Model and some Beyond Standard Model models.

List of Figures

List of Tables

1 Introduction

Since the discovery of the Higgs boson back in 2012, no clear signal of new physics beyond the Standard Model has been observed at the LHC. This has led physicists to increasingly depend on strategies that rely upon theoretical predictions made for known phenomena. Moreover, it implies that particle physics or more precisely hadronic physics is becoming more and more of a high-precision domain. In this context, tools such as event generators like MadGrap5_aMC@NLO [1],[2] have become increasingly influential as physicists turn to known processes to search for new physics [1] .

This Master's thesis focuses on adding features to a tool, MadGrap5_aMC@NLO, designed to provide the theoretical knowledge to be able to look for those deviations between the Standard Model and BSM physics. To be more precise, this work focuses on MadSpin [3], a part of the MadGraph framework used to decay narrow resonances. The term narrow is quite important and is discussed further in section 3.1. MadSpin currently possesses 3 available modes called "None","Onshell" and "Full" made for different purposes that are discussed in detail in section 3. Still, certain interesting processes such as loop induced processes or interferences between the SM and BSM [2] cannot be treated within MadSpin. Hence the need for a new mode that can produce results for such processes. Here the focus does not lie in performance but on providing all the necessary tools to allow such a mode to exist.

To explain the genesis of this new mode called "Density" [3] this Master's thesis first focuses on MadGraph itself. Section 2 focus on how MadGraph usually computes matrix elements which will be the quantity of relevance throughout this Master's thesis. Then section 3 explains how MadSpin uses the MadGraph framework to perform the decay of those narrow resonances. Next, in section 4 MadSpin's Density mode is introduced and the results presented in subsection 4.2. This section finishes with an explanation of the mode's current limitations. Finally, section 5 concludes summing up what was developed throughout this work.

[1] Effective field theories approaches to physics beyond the Standard Model embody such strategies
[2] Loop induced processes are processes for which no tree-level exists.
[3] In reference to the spin density matrix

2 Matrix elements

As stated in the introduction, this first section will focus on MadGraph itself and on the tools it will provide for MadSpin to decay events. MadGraph is designed to generate LHC-like events for which MadGraph also computes the differential cross section using the following Master equation

$$d\sigma_{a,b\to X} = \sum_{a,b} \int dx_1 dx_2 d\phi \;\; f_a(x_1,\mu_F) f_b(x_2,\mu_F) \;\; \sigma_{a,b\to X}(\hat{s},\mu_F,\mu_R) \tag{1}$$

where the integration is done over x_1, x_2, the fractions of momentum taken by each parton, and ϕ a phase space variable. There is also a dependence in μ_F, the scale of the interaction or factorization scale through the PDF's (Parton Distribution Function). The cross section is obtained as a perturbation series in the coupling constant α_s for fixed center of mass energy

$$\sigma(\hat{s},\mu_F,\mu_R) = \sigma_{Born} \times \left[1 + \left(\frac{\alpha_s}{2\pi}\right)\sigma_1 + \left(\frac{\alpha_s}{2\pi}\right)^2 \sigma_2 + O\left(\left(\frac{\alpha_s}{2\pi}\right)^3\right)\right]. \tag{2}$$

Matrix elements, denoted $\mathscr{M}$, are the building blocks used to compute the cross section for fixed order at fixed energy, via the following equation :

$$\sigma(\hat{s},\mu_F,\mu_R) = \frac{1}{2\hat{s}} \int |\mathscr{M}|^2 d\phi(n) \tag{3}$$

where $\hat{s}$ is the energy in the center of mass squared and ϕ is the solid angle in which the particle has been scattered. As shown in the next chapters, the main focus of this Master's thesis consists in the computation of these matrix elements.
This section focuses on how MadGraph usually computes them. I describe MadGraph's approach in two steps. First, I design a possible analytical approach and then explicit the one chosen by MadGraph explaining the differences with the analytical one. The techniques used in the analytical description come again later in this work.

2.1 Trace techniques and Spin Averaged Matrix Elements

To illustrate the theoretical concepts used to design an analytical approach to compute matrix elements, I use, without loss of generality, the example of an electron-positron pair

annihilation producing a muon-antimuon pair (e+ e- > a > mu+ mu-). Using Feynman rules[4] to write the amplitude associated to this process one can write

$$\mathscr{M} = \frac{-e^2}{\hat{s}} g_{\mu\nu} j_e^\mu j_\mu^\nu \tag{4}$$

where the currents j_e^μ, j_μ^ν are defined as

$$j_e^\mu = \bar{v}(p_2)\gamma^\mu u(p_1) \quad and \quad j_\mu^\nu = \bar{v}(p_4)\gamma^\nu u(p_3) \tag{5}$$

To compute the squared amplitude, we use the spin-averaged matrix element i.e. we take the average over all the possible initial helicity configurations and sum over all final state helicities. In the example, each lepton can take two different helicities, +1 or -1[5] meaning 16 possible helicity configurations[6]. Since all 4 initial helicity configurations are equally likely, one can write[7]

$$|\mathscr{M}|^2 = \frac{e^4}{4\hat{s}} \sum_{r,s,r',s'} |\mathscr{M}^{\mu\nu}_{r,s,r',s'}|^2 \tag{6}$$

and

$$\begin{aligned}\sum_{r,s,r',s'} |\mathscr{M}^{\mu\nu}_{r,s,r',s'}|^2 := &\sum_{r,s} \left(\bar{v}(p_2)^r \gamma^\mu u(p_1)^s\right) \left(\bar{v}(p_2)^r \gamma^\nu u(p_1)^s\right)^\dagger \times \\ &\sum_{r',s'} \left(\bar{v}(p_4)^{r'} \gamma_\mu u(p_3)^{s'}\right) \left(\bar{v}(p_4)^{r'} \gamma_\nu u(p_3)^{s'}\right)^\dagger\end{aligned} \tag{7}$$

where the gamma matrices were contracted with the metric and the indices r, s, r', s' indicate the helicity of each particle in the process. The $\frac{1}{4}$ factor accounts for the averaging procedure explained above.

Moreover, the complex conjugate terms in the equation are of the form

$$[\bar{v}\gamma^\mu u]^\dagger := [v^\dagger \gamma^0 \gamma^\mu u]^\dagger = u^\dagger \gamma^{\mu\dagger} \gamma^{0\dagger} v = u^\dagger \gamma^0 \gamma^0 \gamma^{\mu\dagger} \gamma^0 v = \bar{u}\gamma^0 \gamma^{\mu\dagger} \gamma^0 v = \bar{u}\gamma^\mu v \tag{8}$$

[4] Here purely QED

[5] Helicity is the projection of spin on the direction of motion $h := \frac{S \cdot p}{p}$. Hence for spin $\frac{1}{2}$ particles the helicity can only have two eigenvalues $\frac{+1}{2}$ or $\frac{-1}{2}$ i.e. right-handed or left-handed

[6] In the limit $E >> m$, only 4 helicity configurations give non zero values because of the simplifications it induces in the spinors. In this limit, $\frac{p}{E+m} \xrightarrow{E>>m} 1$ and the energy appears only as a global factor in front of each spinors. "Inside" the spinors, only an angular dependance remains.

[7] The underlying assumption is that the beams are unpolarized. However, for lepton colliders it is common to polarize the beams to enhance some processes. Thus in this case, each initial configuration would come with a different weight.

where 3 properties of the gamma matrices where used $\gamma^{0\dagger} = \gamma^0$, $\gamma^0\gamma^0 = \mathbf{1}$ and $\gamma^0\gamma^{\mu\dagger}\gamma^0 = \gamma^\mu$ [8]. Hence, one can write

$$\sum_{r,s,r',s'} |\mathscr{M}^{\mu\nu}_{r,s,r',s'}|^2 := \sum_{r,s} \left(\bar{v}(p_2)^r \gamma^\mu u(p_1)^s\right)\left(\bar{u}(p_1)^s \gamma^\nu v(p_2)^r\right) \times \sum_{r',s'} \left(\bar{v}(p_4)^{r'} \gamma_\mu u(p_3)^{s'}\right)\left(\bar{u}(p_3)^{s'} \gamma_\nu v(p_4)^{r'}\right). \tag{9}$$

The squared amplitude can be decomposed into two terms

$$|\mathscr{M}|^2 = \frac{e^4}{4\hat{s}}\ \mathbf{L}^{e,\mu\nu} \times \mathbf{L}^\mu_{\mu\nu} \tag{10}$$

where $\mathbf{L}^{e,\mu\nu}$ is the left-hand side sum over r and s and $\mathbf{L}^\mu_{\mu\nu}$ is the right-hand side sum over r' and s'. Expliciting the matrix product in the left-hand side sum yields

$$\mathbf{L}^{e,\mu\nu} = \sum_{j,i,n,m} \sum_{r,s} \bar{v}^r_j(p_2)\gamma^\mu_{ji} u^s_i(p_1)\bar{u}^s_n(p_1)\gamma^\nu_{n,m} v^r_m(p_2). \tag{11}$$

Since the sum now contains numbers, they can be ordered as follows

$$\mathbf{L}^{e,\mu\nu} = \sum_{j,i,n,m} \left[\sum_r v^r_m(p_2)\bar{v}^r_j(p_2)\right]\gamma^\mu_{ji}\left[\sum_s u^s_i(p_1)\bar{u}^s_n(p_1)\right]\gamma^\nu_{n,m}. \tag{12}$$

Using the following relations for particles and anti-particles

$$\sum_s u^s_i(p_1)\bar{u}^s_n(p_1) = \not{p_1} + m \qquad \sum_r v^r_m(p_2)\bar{v}^r_j(p_2) = \not{p_2} - m, \tag{13}$$

we obtain

$$\begin{aligned}\mathbf{L}^{e,\mu\nu} &= \sum_{j,i,n,m} \left(\not{p_2} - m\right)_{m,j} \gamma^\mu_{ji} \left(\not{p_1} + m\right)_{i,n} \gamma^\nu_{n,m} \\ &= \sum_m \left((\not{p_2} - m)\gamma^\mu(\not{p_1} + m)\gamma^\nu\right)_{m,m} = Tr\left((\not{p_2} - m)\gamma^\mu(\not{p_1} + m)\gamma^\nu\right).\end{aligned} \tag{14}$$

Similarly, for the muonic part of the matrix element, we find

$$\mathbf{L}^\mu_{\mu\nu} = Tr\left((\not{p_4} - m)\gamma_\mu(\not{p_3} + m)\gamma_\nu\right). \tag{15}$$

[8] See Appendix A for proof

Since MadGraph focuses on generating LHC-like events where all particles are in the ultra-relativistic limit, MadGraph puts all light particle masses [9] to zero, simplifying the expression above. Using the trace properties of gamma matrices

$$Tr\Big(\gamma^\rho\gamma^\mu\gamma^\sigma\gamma^\nu\Big) = 4g^{\rho\mu}g^{\sigma\nu} - 4g^{\rho\sigma}g^{\mu\nu} + 4g^{\rho\nu}g^{\mu\sigma} \tag{16}$$

to find

$$\begin{aligned} Tr\Big((\not{p_1})\gamma^\mu(\not{p_2})\gamma^\nu\Big) &= p_{2,\rho}p_{1,\sigma}Tr\Big(\gamma^\rho\gamma^\mu\gamma^\sigma\gamma^\nu\Big) \\ &= p_{2,\rho}p_{1,\sigma}\Big(4g^{\rho\mu}g^{\sigma\nu} - 4g^{\rho\sigma}g^{\mu\nu} + 4g^{\rho\nu}g^{\mu\sigma}\Big) \end{aligned} \tag{17}$$

and

$$\begin{aligned} Tr\Big((\not{p_4})\gamma_\mu(\not{p_3})\gamma_\nu\Big) &= p^{4,\rho}p^{3,\sigma}Tr\Big(\gamma_\rho\gamma_\mu\gamma_\sigma\gamma_\nu\Big) \\ &= p^{4,\rho}p^{3,\sigma}\Big(4g_{\rho\mu}g_{\sigma\nu} - 4g_{\rho\sigma}g_{\mu\nu} + 4g_{\rho\nu}g_{\mu\sigma}\Big), \end{aligned} \tag{18}$$

combining those two equations keeping in mind that $g^{\mu\nu}g_{\mu\nu} = 4$ and $g^{\rho\sigma}p_{2,\rho}p_{1,\sigma} = p_2 \cdot p_1$, one gets

$$|\mathscr{M}|^2 = \frac{e^4}{4s}\ \mathbf{L}^{e,\mu\nu} \times \mathbf{L}^{\mu}_{\mu\nu} = \frac{8e^4}{s}\Big((p_2\cdot p_4)(p_1\cdot p_3)\Big) + \Big((p_1\cdot p_4)(p_2\cdot p_3)\Big). \tag{19}$$

Now that an analytical description of our problem has been derived, we can try to implement this approach numerically. This should be straightforward as only the momenta's of each particle and the value of the coupling e are needed. In our example, there are two possible Feynamn diagrams associated to the annihilation of an electron-positron pair into a muon-antimuon pair: one where the virtual particle is a photon, the other with a Z boson as the intermediate particle. To compute the total cross section, one needs the squared amplitude associated to the photon, the one associated to the boson and the interference between the diagrams. Thus, three quantities are needed to compute the total cross section. Extrapolating this number for more complex processes, one can find that for a process associated to M diagrams we actually have to compute $\frac{M(M+1)}{2}$ values in this analytical approach.
Although this approach seems quite natural, because of this previous property, MadGraph's

[9] i.e. except bosons, the top, the tau and the b

approach is more suited to a systematic implementation. This is detailed in the next subsection.

2.2 Helicity Amplitudes

The approach used by Madgraph can be summed up in four steps :

(1) Fix the helicity of all external particles and compute $\mathscr{M}_{r,s,r',s'}$

(2) Compute $|\mathscr{M}_{r,s,r',s'}|^2$ by multiplying (1) by $\mathscr{M}^*_{r,s,r',s'}$

(3) Loop on all possible helicity configurations

(4) Average over all possible initial helicity configurations (spin-averaged matrix element)

Going back to the example of section 2.1, one can write the associated matrix element for a given helicity as

$$\mathscr{M}_{r,s,r',s'} = \left(\bar{v}^r(p_2)\gamma^\mu u^s(p_1)\right) \frac{-e^2 g_{\mu\nu}}{s} \left(\bar{v}^{r'}(p_4)\gamma^\nu u^{s'}(p_3)\right). \tag{20}$$

MadGraph then treats each spinor (for given helicity) in this expression as a function $f(p,m)$ of mass and momentum. Next, MadGraph computes the "propagator's wavefunction"

$$W^\nu(\bar{v}(p_4),u(p_3),e,m_p,\Gamma_p) = \frac{e g_{\mu\nu}}{q^2 - m_p^2 + i m_p \Gamma_p} \left(\bar{v}^{r'}(p_4)\gamma^\nu u^{s'}(p_3)\right) \tag{21}$$

where p denotes the intermediate particle. Finally, MadGraph computes the matrix element

$$\mathscr{M}_{r,s,r',s'} = e\left(\bar{v}^r(p_2)\gamma^\mu u^s(p_1)\right) \times W^\nu(\bar{v}(p_4),u(p_3),e,m_p,\Gamma_p) \tag{22}$$

concatenating a current[10] with this wavefunction. Those computations are provided by the HELAS [11] routines [8] and realize the first of the 4 steps in the procedure defined previously. The second step is straightforward and the last two represent the actual computation

[10] the order in which the currents are associated with the propagator is not important

[11] As each step only depends on the spinorial/Lorentz structure of the Feynman rules, whose number is finite for the Standard Model, the Helas routines were invented to provide all possible combination of routines. They were then extended to various models (in particular SUSY) and finally ALOHA [5] automated the routines for any BSM model.

	M Feynman diagrams	N particles
Analytical approach	$\frac{M(M+1)}{2}$	$(N!)^2$
MadGraph approach	M	$N!2^N$

Table 1: Difference in complexity between analytical approach and MadGraph's implementation

of the following expression

$$|\mathscr{M}|^2 = \frac{1}{4} \sum_{r,s,r',s'} |\mathscr{M}_{r,s,r',s'}|^2 \tag{23}$$

where the sum loops over values already computed thanks to the HELAS routines. The figures below display a graphical representation of the procedure used to compute the amplitudes. Thanks to this 4 step procedure, one directly gets the amplitude associated to each diagram when computing the squared amplitude. They do not need to be computed separately. Hence, if there are M diagrams associated to a process, one only needs to compute M different values. The difference in complexity is shown inside table 1.

One can conclude that, by fixing the helicity and computing the squared amplitudes using blocks provided by the HELAS routines, MadGraph is able to do better than an analytical approach to compute matrix elements if N or M is large enough [12].

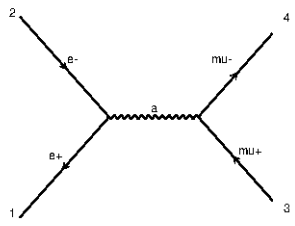

Figure 1: Feynman diagram associated to the electron-positron annihilation

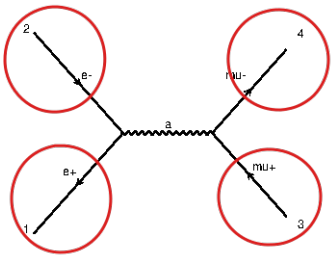

Figure 2: First, the spinors (for a given helicity configuration) are computed for each external particle

[12] In practice, it is better for $2 > 4$ processes

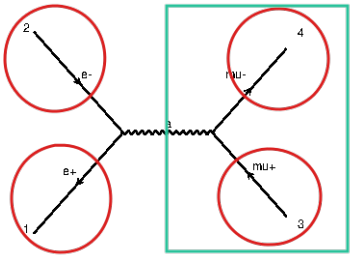

Figure 3: The "propagator's wavefunction" is computed as in equation (27)

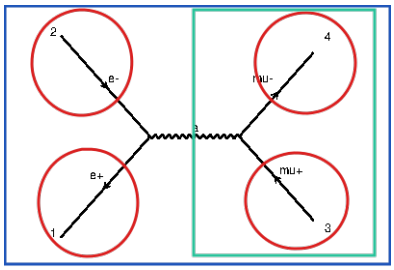

Figure 4: Finally, the blocks are put together to compute the whole matrix element for a given helicity configuration as in (28)

3 Madspin

As stated in the introduction, MadSpin is a method within the MadGraph framework used to decay narrow resonances. The term *narrow* is used to refer to the Narrow Width Approximation (hereafter, NWA), that is, the width of the particle, $\Gamma << M$, is significantly smaller than its onshell mass. In this regime one can treat a diagram such as in figure 1 cutting it in two parts, "production" and "decay"[13]. If a particle is not in this regime, say very low in mass and very offshell, one could end up with processes with a photon instead of the decaying particle. Yet, photons are massless and thus, have a pole in their squared amplitude yielding abnormally high values far from the onshell mass of the resonance. This is the reason why the NWA assumption is crucial. The next point will be dedicated to a detailed explanation of the implications of this assumption.

3.1 Narrow Width Approximation

As stated in [9], perturbative computations involving unstable particles in Quantum Field Theory can be quite complicated. This section will focus on how to treat such particles when their width Γ is much smaller than their mass M. As will be shown in this section, this limit allows to forget about the non-resonant and non-factorizable parts of a given diagram. The proof will be done for a two body decay but a generalization can be found in [9]. Following the notation of [6] where P accounts for all the incoming particles, D denotes the decaying particle, d_1 and d_2 are the decay products and finally $d_3, \ldots, d_n$ is a

[13] "production" where the decaying particle is produced and "decay" where the decay happens

list associated to all the other final state particles, the process of interest is

$$P \longrightarrow D(\rightarrow d_1 + d_2) + d_3 + ... + d_n. \tag{24}$$

The associated diagram is illustrated in figure 5. Starting from the following generalization of the cross section formula (13) for an unstable particle

$$\sigma(\hat{s}, \mu_F, \mu_R) = \int |\mathscr{M}|^2 D(q^2)\, d\phi_n(P, q, p_{d_1}, p_{d_2}, p_{d_3}, ..., p_{d_m}) \tag{25}$$

where P denotes the sum of the four momenta's of the incoming particles, q the four momentum of the decaying particle, p_{d_1} and p_{d_2} are the four momenta's of the decay products and $p_{d_3}, ..., p_{d_m}$ the four momenta's of the other final state particles. The denominator is

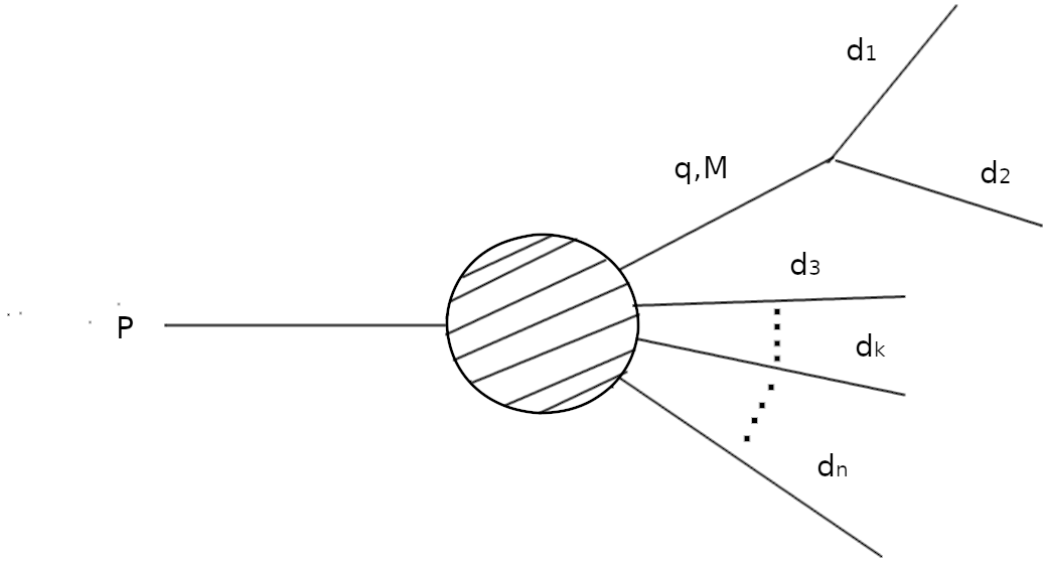

Figure 5: Diagram of interest of a two-body decay and $n-3$ final state particles not associated with the decay

the squared propagator for the unstable particle defined as $D^2(q^2) := \frac{1}{(q^2-M^2)^2+M^2\Gamma^2}$ and $\mathscr{M}$ here is the matrix element from which the denominator D has been subtracted. Finally, the phase space variable for a n particle phase space element can be written, for a generic case, as follows

$$d\phi_n(P, p_1, ..., p_n) = (2\pi)^4 \delta^4\left(P - \sum_{i=1}^{n} p_i\right) \prod_{k=1}^{n} \frac{d^3\vec{p}_k}{(2\pi)^3 2E_k}. \tag{26}$$

Here in this case one can factorize production and decay

$$d\phi_n(P,q,p_{d_1},p_{d_2},p_{d_3},...,p_{d_m}) = d\phi_j(P,p_{d_3},...,p_{d_{n-3}},q)\ \frac{dq^2}{2\pi}\ d\phi_{n-j+1}(q,p_{d_1},p_{d_2}) \quad (27)$$

where there is a $(n-2)$-particle phase space element for production and there is a 3-particle phase space element for decay. Moreover, there is an integration over the four-momentum of the decaying particle to allow this decomposition. The denominator D can be integrated out in the following way

$$\int_{-\infty}^{\infty} \frac{dq^2}{2\pi} D^2(q^2)\sigma(q^2) \approx \frac{1}{2\Gamma M}\int_{-\infty}^{\infty} \delta(q^2-M^2)\ \sigma(q^2) = \frac{\sigma(M^2)}{2\Gamma M} \quad (28)$$

where first the NWA assumption was made to write the integrand in the asymptotic limit $\Gamma \to 0$ and then the Dirac delta was used to perform the integration.

This simplifies the expressions for the cross section but is not enough to completely factorize production and decay in any full diagram. In fact, the limit $\Gamma \to 0$ is not enough because production and decay are still linked by spin correlations. One can say that the process in 24 has spin correlations at the decay level if the matrix elements of the corresponding Feynman diagrams have a non-trivial dependence in $(d_1 \cdot d_2)$. Similarly, this process has spin correlations at the production level if the associated matrix elements have a non-trivial dependence in $(d_i \cdot P)$ or $(d_i \cdot d_k)$ for $i \in \{1,2\}$ and $k \in \{3,..,m\}$. Evidently, if the particle D has non-zero spin, there will always be decay spin correlations.

In practice, it means that one cannot have any factorization at the matrix elements level if all spin correlations are to be retained. Thus, in order to do that, a further assumption needs to be made. This assumption is the factorization of the amplitudes squared between production and decay [14] and can be written in the following way

$$\begin{aligned} |\mathscr{M}_{full}|^2 = |M_p^\mu\ P_{\mu\nu}\ M_d^\nu|^2 &= |M_p^\mu \sum_\lambda \varepsilon_\mu^\lambda \varepsilon_\nu^\lambda\ M_d^\nu|^2 \\ &\approx \sum_{\lambda_1} |M_p^\mu \varepsilon_\mu^{\lambda_1}|^2 \times \sum_{\lambda_2} |M_d^\nu \varepsilon_\nu^{\lambda_2}|^2 =: |\mathscr{M}_{NWA}|^2 \end{aligned} \quad (29)$$

where the propagator has been expressed as a sum over its polarization states and the last step is the new approximation made. Clearly, following the definition of spin correlation, this approximation can account for decay spin correlations but not for production ones.

[14] Called the decay chain approximation in [6]

Moreover, one can prove that, taking the limit $\Gamma \to 0$, computing 3 using M_{full} or $\mathscr{M}_{NWA}$ actually yields the same results. This means that in this limit, one can factorize production and decay without affecting the results. The proof of this statement can be found in appendix B.

3.2 MadSpin Modes

There are currently 3 different modes implemented in MadSpin, each of them having their own ways of working and capabilities. I will now describe them, their use cases as well as their limitations.

3.2.1 MadSpin Mode : NONE

The "none" mode is the most basic one. The procedure used is the following

(1) Generate production events with the resonance on its mass shell

(2) Generate decay events in the rest frame of the resonance

(3) Merge the production and decay events

In this mode, no information from production is used to generate the decay events. Hence, all possible correlations are completely lost. There are no correlations between the resonance and the decay products since they are generated completely independently. This mode is very well suited to the decay of the Higgs since it is a spin 0 particle, i.e. they are no spin correlations between production and decay. The width of the Higgs is also extremely narrow and they are no real offshell effects that need to be accounted for. As such, the goal of this Master's thesis is also to provide another option for cases in which the "none" mode is the only one available but they are spin correlations to keep.

3.2.2 MadSpin Mode : ONSHELL

The "onshell" mode aims at keeping correlations at the decay level i.e. between the resonance and its decay products. This is done using an accept/reject procedure :

(1) Generate production events with the resonance on its mass shell

(2) For each production event, generate unweighted decay events in the rest frame of the resonance

(3) Accept/reject procedure. Decay events are accepted if :

$$\frac{d\phi_n \;\; f_a(x_1,\mu_F) f_b(x_2,\mu_F) \; |\mathbf{M}_{full}|^2}{d\phi_{n-3} \;\; f_a(x_1,\mu_F) f_b(x_2,\mu_F) \; |\mathbf{M}_{Prod}|^2 \times d\phi_3 \; |\mathbf{M}_{Decay}|^2} = \frac{|\mathbf{M}_{full}|^2}{|\mathbf{M}_{Prod}|^2 \times |\mathbf{M}_{Decay}|^2} > rW_{max} \tag{30}$$

where $d\phi_n$ is a little n-elements phase space volume associated to the full event i.e. "production" + "decay". The left-hand side term is the weight associated to each decay event. The numerator is the density probability i.e.for the full event and is computed at Leading Order (hereafter, LO). However, since a production and a decay events were generated, there is the need to divide the weight by the density probability of having those events. This is what is done at the denominator, at LO just as the numerator [15]. The second step is obtained by noting that the phase space volume associated to production and decay combined with each other actually gives the full phase-space volume. Thus, they cancel as well as the PDF's and this is shown in the second step of the equation above.

The right-hand side term consists of a random number r$\in [0,1]$ generated at each accept/reject and a maximum W_{max}. This maximum can be proven to always exist in the NWA and was originally given analytically in [6]. Here, it is a numerical approximate that will be computed as follows

- For the m first production events, probe the phase space of the decay with a large number of points and extract the maximum W. The maximum associated to the i^{th} production event is denoted W_i for $i \in [1,...,m]$
- Draw a Gaussian associated to all of those maxima :

$$W_{max} = \langle W_i \rangle + \xi \; std(W_i)$$

where ξ is an empirical parameter adjusted to be as close as possible to the real maximum.

(4) Merge production and decay events, if accepted, to obtain the desired full event or

[15] One can note that the production event generated in step (1) was computed at NLO accuracy and the accept/reject procedure only at LO. Thus there is a loss of accuracy happening there. If loop induced processes can become available using the Density mode, one could hope to recover some NLO effects even tough it wouldn't be straightforward.

repeat procedure from (2).

In this mode, spin correlations between production and decay are kept at LO accuracy since decay events are accepted only if the probability associated to the full event ("production" + "decay") is close to being maximized.

3.2.3 MadSpin Mode : FULL

The "full" mode, the last available mode in MadSpin, aims at preserving spin correlations at the decay level while accounting for finite width effects. This procedure is slightly different from the previous one

(1) Generate production events with the resonance on its mass shell

(2) For each production event :

- For each channel of integration i, compute the associated branching $w_i = \frac{|M_i|^2}{\sum_j |M_j|^2}$
- Choose one channel of integration randomly with a weight w_i for each channel
- Generate phase space points for the decay products according to a uniform distribution in the rest frame of the decaying particle. Generate the virtuality of the resonance according to a Breit-Wigner. To avoid conflicts with the NWA, MadSpin has a default cut-off that can be changed manually. This cut-off avoids cases where the resonance is extremely offshell.

(3) Accept/reject procedure. Decay points are accepted if :

$$\frac{|\mathbf{M}_{full}|^2}{|\mathbf{M}_{Prod}|^2} > rW_{max}\,[16].$$

Unlike the "onshell" mode, the probability for the decay event is absent from the denominator due to the fact a decay event is not generated while phase space points are. Moreover, as for "onshell", the full and production matrix elements are computed at tree level. The maximum, W_{max}, is computed as in subsection 3.2.2.

(4) If the inequality is not satisfied, repeat the procedure starting from point (3).

[16] Here the cancellations of 30 are less obvious as allowing the resonance to be slightly offshell can change the arguments of the PDF's. In practice this happens only for 2 > 1 processes such as p p > H.

In this mode, the spin correlations are kept exactly in the same way as in the "onshell" mode except that the kinemetics of the full event allow some virtuality for the resonance. This was done by smearing the mass of the resonance according to a Breit-Wigner.

3.3 Remarks

Historically the goal of MadSpin is to decay resonances at NLO. When doing so, MadSpin uses the full event generated by MadGraph. The key point is that MadSpin only needs it at LO to preserve spin correlations [17]. Thus, this is the advantage MadSpin has over asking MadGraph for the full event every time.
Nonetheless, some knowledge about the full event is needed when performing the accept/reject procedure. This means that if, as for loop-induces processes or interferences, a process is not available in MadGraph, the "onshell" and "full" modes cannot give any results since they are not capable of computing the full matrix element. Thus, designing a way of computing matrix elements that only requires the knowledge of the production and decay events while preserving spin correlations would be useful. This is the focus of this Master's thesis.

4 MadSpin's Density Mode

This section is dedicated to the derivation of MadSpin's density mode. This new mode aims at computing matrix elements in a different way to consistently yield results for every process for which production and decay parts are known separately. This is done in four subsections. The first treats the way the density mode computes matrix elements and highlights why it is different than what was done within MG5aMC until now. Subsection 4.2 is dedicated to the validation of those computations for several processes. Finally, this section ends with a review of this mode's current limitations.

4.1 Theory

This section is divided in two parts. First, deriving the Master formula for a colorless resonance, second, the general case where color is considered. This allows to really see the basic concepts used.

[17] Full NLO would yield better results but would also be a lot more expensive

4.1.1 Colorless Resonance

As before, the NWA is crucial to treat production and decay separately except that now, one looks directly at the amplitude level

$$\mathscr{M} = \mathscr{M}_\mu^P P^{\mu\nu} \mathscr{M}_\nu^D \tag{31}$$

where $P^{\mu\nu}$ accounts for the propagator between the production amplitude and the decay one. For bosons $P_{\mu\nu} = -g_{\mu\nu} + \frac{q_\mu q_\nu}{M^2} = \sum_\lambda (\varepsilon_\mu^\lambda)^* \varepsilon_\nu^\lambda$ and for fermions $P_{\mu\nu} = \not{q} + M = \sum_{s,s'} u_s \bar{u}_{s'}$ where in the last step, the propagator has been expressed as a sum over its polarization states for the spin-1 bosons as in 3.1 and over the spinor's hecilicities for fermions [18]. Writing the squared matrix element choosing the case of a spin-1 boson for now on, yields

$$\mathscr{M} = \mathscr{M}_\mu^P \left(\sum_\lambda (\varepsilon_\lambda^\mu)^* \varepsilon_\lambda^\nu \right) \mathscr{M}_\nu^D. \tag{32}$$

As in section 2.1, taking the spin-averaged matrix element, one gets

$$|\mathscr{M}|^2 = \frac{1}{f} \sum_{s,s'} \left| \mathscr{M}_{\mu,s}^P \left(\sum_\lambda (\varepsilon_\lambda^\mu)^* \varepsilon_\lambda^\nu \right) \mathscr{M}_{\nu,s'}^D \right|^2 \tag{33}$$

where f is the number of possible initial helicity configurations times the number of color configurations [19] for the incoming particles. As stated in section 2.1, the spin-averaged technique also involves a summation over final state helicities. Moreover, for spin-1 bosons, there are 3 onshell polarization states defined, following [8], for four-momentum $k^\mu = (E, k_x, k_y, k_z)$ as

$$\varepsilon_1^\mu = \frac{1}{|\vec{k}| \times k_T} \left(0, k_x k_z, k_y k_z, -k_T^2 \right) \tag{34}$$

$$\varepsilon_2^\mu = \frac{1}{k_T} \left(0, -k_y, k_x, 0 \right) \tag{35}$$

$$\varepsilon_3^\mu = \frac{E}{|\vec{k}| \times M} \left(\frac{|\vec{k}|^2}{E}, k_x, k_y, k_z \right) \tag{36}$$

where $M = \sqrt{E^2 - |\vec{k}|^2}$ and $k_T = \sqrt{k_x^2 + k_y^2}$. There is also an additional offshell component i.e. non-zero if the resonance is not on its mass shell. As in [4], this auxiliar state can be

[18] Note that for a spin 0 particle, there are no such sums as there are no helicities or polarizations available

[19] If the particle has color

written as

$$\varepsilon_4^\mu = \frac{k^\mu}{M}\sqrt{\frac{k^2 - M^2}{k^2}}. \tag{37}$$

This auxiliar state is currently not available in MadGraph and the sums over the polarization state index λ will only contain the onshell parts ε_k^μ for $k \in \{1,2,3\}$. As will be shown in the validation section, this does not introduce large errors when considering a slightly offshell resonance [20]. Similarly, in the case of a fermionic resonance, the offshell conributions are not accounted for but the validation section will assure us that the procedure still gives good results even when the resonance's invariant mass is different than its onshell one.
The big difference with the expression 33 compared to the definition of $\mathscr{M}_{NWA}$ of equation 29 is the fact production and decay share indices, λ and λ', associated to the resonance's polarization states. Those interferences between production and decay are missing in the decay chain approximation introduced in 3.1. This main difference comes up again when considering the general case.

4.1.2 General Case

To derive a general Master equation, the resonance should be allowed to have color. In this context, standard computations such as in [7] perform a color decomposition of the matrix elements. Several color basis on which the decomposition is performed can be chosen such as the fundamental one or the color-flow basis. Such a choice will be irrelevant as computations are quite general. One can write this decomposition for a color coefficient F in the following manner

$$\mathscr{M} = \sum_{a,b} F^{a,b}\mathscr{M}_{a,b}. \tag{38}$$

Here there are two indices for colour. The first one, a, is a list of indices for all particles in the process except the resonance for which there is another index, called b. The reason of this choice becomes clear when deriving the formula. First, introducing color into the usual way MadGraph computes matrix elements i.e. as in 29 using the NWA and the decay

[20] And the resonance will always be slightly offshell or onshell as we consider the NWA

chain approximation, one gets

$$|\mathscr{M}_{full}|^2 = \left| \sum_{a,b} F^{a,b} \mathscr{M}^P_{\mu;a,b} \, P^{\mu\nu} \sum_{c,d} P^{c,d} \mathscr{M}^D_{\nu;c,d} \right|^2 \tag{39}$$
$$\approx \sum_{\lambda_1} \left| \sum_{a,b} F^{a,b} \mathscr{M}^P_{\mu;a,b} (\varepsilon^\mu_{\lambda_1})^* \right|^2 \times \sum_{\lambda_2} \left| \sum_{c,d} P^{c,d} \mathscr{M}^D_{\nu;c,d} \, \varepsilon^\nu_{\lambda_2} \right|^2 .$$

Introducing the colored ordered amplitudes $\mathscr{J}$, also called JAMP's [21], as

$$\mathscr{J}^P_{\lambda;,a,b} := \mathscr{M}_{\mu;a,b} \, (\varepsilon^\mu_\lambda)^* \;\; , \;\; \mathscr{J}^D_{\lambda;,c,d} := \varepsilon^\nu_\lambda \, \mathscr{M}^D_{\nu;c,d} \tag{40}$$

and introducing the color matrices $\mathbf{C}$ and $\mathbf{C}'$ which are defined in the following way

$$\mathbf{C}^{a,b;a',b'} := F^{a,b} \times (F^{a',b'})^* \;\; , \;\; \mathbf{C}'^{c,d;c',d'} := P^{c,d} \times (P^{c',d'})^*, \tag{41}$$

one can write the full matrix elements squared as

$$|\mathscr{M}_{full}|^2 = \sum_{\lambda_1,\lambda_1'} \left[\sum_{a,b,a',b'} \mathbf{C}^{a,b,a',b'} \, \mathscr{J}^P_{\lambda_1;a,b} (\mathscr{J}^P_{\lambda_1';a',b'})^* \right] \times \tag{42}$$
$$\sum_{\lambda_2,\lambda_2'} \left[\sum_{c,d,c',d'} \mathbf{C}'^{c,d,c',d'} \, \mathscr{J}^D_{\lambda_2;c,d} (\mathscr{J}^D_{\lambda_2';c',d'})^* \right].$$

This is the standard approach used by MadGraph to compute matrix elements forgetting about the spin-averaged techniques for comparison purposes.
Doing the same procedure as previously, but now following the decomposition into production and decay at the amplitude level of 4.1.1, one finds

$$\mathscr{M} = \sum_{a,b,c,d} \left(F^{a,b} \mathscr{M}^P_{\mu;a,b} \right) \left(\sum_\lambda (\varepsilon^\mu_\lambda)^* \varepsilon^\nu_\lambda \delta^{b,c} \right) \left(P^{c,d} \mathscr{M}^D_{\nu;c,d} \right) \tag{43}$$

where a Kroenecker delta appear because of color conservation and b and c are the indices associated to the decaying particle. Using the definitions 40 and 41 of the JAMP's and the

[21] This is how they are called in the code

color matrices to write the squared amplitude, one gets

$$|\mathscr{M}|^2 = \sum_{\lambda_1,\lambda_2} \left[\sum_{a,b,a',b'} \mathbf{C}^{a,b,a',b'} \mathscr{J}^P_{\lambda_1;a,b} (\mathscr{J}^P_{\lambda_2;a',b'})^* \right] \times \delta^{b,c} \delta^{b',c'} \times \left[\sum_{c,d,c',d'} \mathbf{C}'^{c,d,c',d'} \mathscr{J}^D_{\lambda_1;c,d} (\mathscr{J}^D_{\lambda_2;c',d'})^* \right]. \tag{44}$$

The big difference between this way of computing matrix elements and MadGraph's usual way is the fact that the sum over λ_1 and λ_2 involves both production and decay. In 42 the interference term between production and decay are missing. Moreover, Kroenecker delta's also appear to render color conservation. These are not present in 42 due to the decay chain approximation. In 44, production and decay are not treated as two distinct objects anymore. As will become clear in the next section on the validation procedure, the Kroenecker delta's incorporating the color conservation are not practical, as they make a link between production and decay directly in the color sums while, using MadGraph, one can only recover information about production and decay separately at this color level. What is possible using MadGraph, is computing these color sums inside the parenthesis for production and decay separately. To bypass this problem and forget about the Dirac delta's, one can say that, since all the elements that possess a color index here are invariant under SU(3), the terms inside the color sums are invariant under SU(3) and one can remove the Kroenecker delta's by dividing by the number of color. In other words, there should not be a sum over c and c' because of the Kroenecker delta's, but the choice is to compute them regardless, remove the delta's and divide by the number of colors as the term inside the sum is invariant under SU(3). This argument will also be checked in the next section when performing the actual validation. Hence, re-introducing the spin-averaged matrix element, the Master equation becomes the following one

$$|\mathscr{M}|^2 = \frac{1}{N_c \times f} \sum_{\substack{s_1,s_2 \\ s'_1,s'_2}} \left[\sum_{\lambda_1,\lambda_2} \underbrace{\left(\sum_{a,b,a',b'} \mathbf{C}^{a,b,a',b'} \mathscr{J}^P_{\lambda_1,s_1;a,b} (\mathscr{J}^P_{\lambda_2,s'_1;a',b'})^* \right)}_{\text{INTER PRODUCTION}} \times \underbrace{\left(\sum_{c,d,c',d'} \mathbf{C}'^{c,d,c',d'} \mathscr{J}^D_{\lambda_1,s_2;c,d} (\mathscr{J}^D_{\lambda_2,s'_2;c',d'})^* \right)}_{\text{INTER DECAY}} \right] \tag{45}$$

where N_c is the resonance's number of colors and the JAMP's have been upgraded by an

additional index which refers to the helicity sum associated to the spin-averaged technique. The two underlined terms called $INTER$ are the color sums. They turn out to be important in the next section dedicated to the validation of this formula through various processes for which Madgraph already gives good results.

4.2 Validation

4.2.1 Validation procedure

As stated previously, this sections focuses on the validation of equation 45 for several processes, trying to be as exhaustive as possible to convince oneselves that the argument to drop the delta's works and also to see if the implementation of formula 45 is ready to be taken into the MadSpin framework. This is done by computing the matrix element using equation 45 for processes for which MadGraph already gives good results and then comparing the results obtained with the results given by MadGraph. Evidently, the goal is to obtain ratios equal to one up to a precision of the order of numerical fluctuations.
Those tests are done using MadGraph standalone mode. This mode allows users to generate events and put all the dependencies used for this generation in their own separate compartmentalized folders. In each of these standalone folders, the interesting scripts are in "$matrix.f$", a Fortran script in which all the routines used to compute matrix elements are stored. The comparison of both ways of computing matrix elements involves adding routines in this Fortran script. The exact procedure is the following

(1) For a particular process, generate production and decay events in standalone mode.

(2) For both production and decay, add a routine called GET_INTER in "$matrix.f$" to compute the $INTER$ defined in equation 45. This routine gives as output a matrix in which each entry is associated to one helicity+polarization configuration, i.e. for one choice of $s_1, s_1', \lambda, \lambda'$ if it is for production. This is why the kroenecker delta's were not practical. One wants to add routines in each standalone mode which are separate and use double precision rather than using $F2PY$ [22] which enables making all computations at the same time but without the Fortran advantages. The division by the number of color allows to do the computation of $INTER$ directly in "$matrix.f$". One also needs to retrieve all possible helicity+polarization configurations for both

[22] As stated in their guide, the purpose of the F2PY,"Fortran to Python interface generator" is to provide a connection between Python and Fortran.

production and decay. This can be retrieved directly from "$matrix.f$" adding a small routine.

(3) Using $F2PY$, write a python script retrieving the matrix $INTER$ for both production and decay as well as all their possible helicity+polarization configuration and then compute the matrix element using equation 45. Since the $INTER$ terms were computed before, this step involves performing a convolution.

(3) Generate the full event i.e. production + decay in standalone mode.

(4) In the same python script, use $F2PY$ to utilize the routine GET_VALUE in "$matrix.f$" to get the matrix element computed the usual way by MadGraph. This routing is already implemented and available within MadGraph.

(5) Compute the ratio between both methods for a particular momentum configuration. One can also, making some simple changes in some routine in $matrix.f$, compare matrix elements for each helicity configuration rather than only the full one after the summation over helicity indices.

Now that the validation procedure has been described, the next point focuses on the actual checks for processes for which the formula 45 has been tested.

4.2.2 W boson decay following production of W_+jj

The first case considered is the one of a colorless resonance, encoded by the following process

$$pp > w_+ jj \ , \ w_+ > d_1 \ d_2 \tag{46}$$

where two jets have been produced along with the W boson which then decay into a couple d_1 and d_2 which could be $e+$ and ν_e or a quark-antiquark pair. This check, as do the others, consists in 2 steps. The first step follows the procedure 4.2.1 and focuses on obtaining a ratio equal to one between both methods explained in 4.1.2 for processes that are included in the MadGraph framework. The second step consists in using MadAnalysis5 [23] to produce plots of chosen observables [24].

[23] As stated on their github page, "MadAnalysis 5 is a framework for phenomenological investigations at particle colliders. Based on a C++ kernel, this program allows to efficiently perform, in a straightforward and user-friendly fashion, sophisticated physics analyses of event files such as those generated by a large class of Monte Carlo event generators". In practice this is used to produce plots of interesting observables.

[24] Of course, this procedure does not follow the timeline of the implementation. First, the ratios associated to each process are computed to make sure the procedure works. Then, it is implemented within MadSpin to

Of course, those observables are associated to the kinematics of the decay products as no differences in the production kinematics, between the different modes, is expected. The two observables to be plotted are the transverse momentum and the pseudorapidity of the decay products. The definition of the transverse momentum is quite straightforward and is the following

$$\vec{p}_t = (p_x, p_y) \quad and \quad p_t^2 = p_x^2 + p_y^2$$

where it is assumed that the direction $\hat{z}$ is the direction of the beam. More intuitively, this is the particle's momentum in the direction of the detector if one assumes that the detector is perpendicular to the direction of the collision. This observable is important as one always want to have observables invariant under a boost in the direction $\hat{z}$ of the beam. This prevents two identical events that were $\hat{z}$-boosted differently to appear in different bins when producing histograms. Moreover, looking at the transverse direction, one can expect to have cleaner samples associated to the hard collision as there would be less noise associated to gluons and virtual quarks. This observable is also quite important when the detector has a certain angular resolution [25]. In practice, this means that one can only easily recover information associated to this transverse plane as the resolution does not allow to look in the direction of the collision. By way of an example, this makes this observable crucial to reconstruct the transverse mass of a W boson.

To define the pseudorapidity, we first need to define the standard rapidity. The rapidity is defined as

$$y = \frac{1}{2} ln\left(\frac{E + p_z}{E - p_z}\right) \tag{47}$$

and is an angle associated to each particle in the process. In the case of a massless particle, if the particle is going along the beam, then p_z will be close to E and $y \to \infty$. However, if this particle is directed towards the plane XY, the contribution from p_z will be extremely small and $y \to 0$. Hence, this is a good measure of the direction of the angle between the XY plane and the direction of motion of the product of a hard collision. This measure has the advantage that differences between rapidities are invariant under Lorentz boosts in the beam's direction $\hat{z}$. This is why, sometimes, the rapidity is paired up with the azimutal angle ϕ, the angle between the particle and the beam's direction, to characterise the particle's angular coordinates thus using (y, ϕ). This way, the angular separation between two objects

produce the plot. Here, the plots are shown alongside the ratios.

[25] As it is the case of muon chambers.

Helicity Configuration	$\sum_{\lambda_1,\lambda_2} I^P_{\lambda_1,\lambda_2} \times I^D_{\lambda_1,\lambda_2}$	$\mathscr{M}_{s,s',r,r'}$	Ratio
[-1, -1, -1, 1, -1, -1]	40.90212814356056	40.90212064369881	1.0000001833611958
[-1, 1, -1, 1, 1, -1]	13.684384322821163	13.68438176432162	1.0000001869649349
[1, -1, -1, 1, 1, -1]	1.3089785883215468e-10	1.3089782755853626e-10	1.0000002389162526

Table 2: Non-zero matrix elements for fixed helicity in the case of the decay of a w boson into a quark-antiquark pair. The helicity

is invariant under a Lorentz boost along the beam's axis. This can be particularly useful when considering a process such as $pp > w_+ jj$ as the two jets are expected to be boosted along the $\hat{z}$-direction due to the composite nature of protons [26].

However, the rapidity is not a practical observable when dealing with ultra-relativistic particles, as one needs both energy and the momentum in the $\hat{z}$-direction. Going into spherical coordinates yields $p_z = |\vec{p}|\ cos(\theta)$ and in the ultra-relativistic limit, $E^2 = |\vec{p}|^2$. Hence, one can write the rapidity, in this limit, as

$$\begin{aligned} y &\approx \frac{1}{2} ln\left(\frac{E \times (1+cos(\theta))}{E \times (1-cos(\theta)}\right) \\ &= \frac{1}{2} ln\left(\frac{cos^2\left(\frac{\theta}{2}\right)}{sin^2\left(\frac{\theta}{2}\right)}\right) \\ &= \frac{1}{2} ln\left(cot^2\left(\frac{\theta}{2}\right)\right) \\ &= -ln\left(tan\left(\frac{\theta}{2}\right)\right) =: \eta \end{aligned}$$

where the last line defines the pseudorapidity η. This observable provides a quicker and easier way to characterise the angular dependence of a particle than the rapidity, as less information is needed to compute it. Moreover, both observables coincide in the ultra-relativistic limit which often applies at the LHC.

Now that both observables are defined and explained, one can focus on the actual checks. Those will be done generating 200000 events in each case.

The results from the procedure described in 4.2.1 in the case of 46 for a W decaying into a quark-antiquark pair are shown in table 2 and 3. All phase space points that were used to derive those ratios can be found in appendix C. In table 2, the first column is the helicity

[26] Since, at LHC, collision happen in the center of mass frame of the pp system, the colliding partons insisde the proton have a net longitudinal momemtum equal tp $(x_1 - x_2) \times E$ where the x_1 and x_3 are the colliding partons fraction of energy. Consequently, the two jets are boosted along the $\hat{z}$-direction.

u u $> w_+$ u d$\sim$, $w_+ >$ u d$\sim$	Total Matrix Element Squared	Ratio
MadGraph	54.586502408151325	1.0000001842646231
MadSpin Density	54.586512466512616	

Table 3: Total matrix element squared for the decay of a w boson into a quark-antiquark pair

configuration for which the matrix element is computed, i.e. it is the following term, in the case of the density mode, that is being computed

$$\sum_{\lambda_1,\lambda_2} I^P_{\lambda_1,\lambda_2} \times I^D_{\lambda_1,\lambda_2}$$

where

$$I^P_{\lambda_1,\lambda_2} = \sum_{\lambda_1,\lambda_2} \left(\sum_{a,b,a',b'} \mathbf{C}^{a,b,a',b'} \mathscr{J}^P_{\lambda_1,s_1;a,b} (\mathscr{J}^P_{\lambda_2,s'_1;a',b'})^* \right)$$
$$I^D_{\lambda_1,\lambda_2} = \sum_{\lambda_1,\lambda_2} \left(\sum_{c,d,c',d'} \mathbf{C}'^{c,d,c',d'} \mathscr{J}^D_{\lambda_1,s_2;a,b} (\mathscr{J}^D_{\lambda_2,s_2;c',d'})^* \right).$$

The results are shown in the second column. The third column shows the results for the usual MadGraph computations, i.e. the matrix element squared fixing the helicity of the external particles that can be retrieved in the Fortran routines of "*matrix.f*". Finally, the last column gives the ratio between methods for each helicity configuration. Only non-zero matrix elements are shown here as there are 64 possible helicity configuration [27]. The reason why not all helicity configuration give non-zero value for the associated matrix element is due to the fact MadGraph puts all light particles masses [28] to zero simplifying the expression of the spinors, thus yielding zero for the associated matrix element for a large number of configurations. But this is not the only reason as interactions with the W is pure left and some configurations are not allowed due to energy-momentum conservation. Table 3 gives the sum over all fixed helicity squared amplitudes, hence the total matrix element, for both methods and their ratios.

As one can easily see, both methods give the same results up to a good precision. However, if they were only numerical fluctuations, there should be a difference of the order of 10^{-15} which is not the case here. This difference can be due to the loss of double precision when

[27] Each final state particle has two possible helicities here.

[28] In fact, all particles masses are zero except the tau, b and top quarks, the Z,W's and the Higgs bosons.

Helicity Configuration	$\sum_{\lambda_1,\lambda_2} I^P_{\lambda_1,\lambda_2} \times I^D_{\lambda_1,\lambda_2}$	$\mathscr{M}_{s,s',r,r'}$	Ratio
[-1, -1, -1, 1, -1, -1]	0.0004134386514897463	0.00041343865235403594	0.9999999979095093
[-1, 1, -1, 1, 1, -1]	1.1915374044549637e-13	1.191537406847713e-13	0.9999999979918807
[1, -1, -1, 1, 1, -1]	1.5574170296750047e-06	1.5574170330783162e-06	0.9999999978147719

Table 4: Non-zero matrix elements squared for fixed helicity in the case of the decay of a slightly offshell w boson into a quark-antiquark pair

u u > w_+ u d~, w_+ > u d~	Total Matrix Element Squared	Ratio
MadGraph	0.000414996069506268	0.999999997909154
MadSpin Density	0.00041499606863857507	

Table 5: Total matrix element squared for the decay of a slightly offshell w boson into a quark-antiquark pair

performing the convolution in Python rather than Fortran. Nonetheless, the results match closely.

As stated in 4.1.1, the offshell contributions that could arise if the resonance is slightly off its mass shell are not accounted for in 45, as the auxiliar state is currently not implemented into the routines belonging to "$matrix.f$". Thus, one can only recover the $JAMP's$ associated to ε_k^μ for $k \in \{1,2,3\}$. One could then ask if those offshell contributions are large and if in this case, formula 45 still gives good results. This was carried out and the results are shown in table 4 and 5. Looking at the results, one can say that even for a slightly offshell W, the precision of the method does not change and the effects of the offshell components cannot be seen. To be precise, looking at the auxiliar state 37, this offshell component should cancel in the massless limit and is proportional to the offshelness of the resonance. Here, the invariant mass of the W was $M_W = 84.22074210423051$ which is quite big considering that the width of the W is equal to 2.047600 ans its mass to 80.419002445756163. This gives an indication that the method can still be used even in this case.

As explained previously, the next step is now to produce plots of the transverse momentum and pseudorapidity for each decay product and compare the results between the different modes. This is shown in figures 6-7 for the transverse momenta's and in 8- 9 for the pseudorapidity[29]. One can directly see that the "none" mode gives very different results

[29]The error bars were computed assuming a Poisson distribution for each observable for which the error in each bin is approximately the square root of the number of events within it. One also has to be careful to the fact that MadAnalysis imposes a value of 10 fb^{-1}. Thus, to compute the errors one has to multiply the number of events by the ratio between the real luminosity and the one MadGraph uses to obtain the real number of events in each bin.

than the other available modes that are "full", "onshell" and "density". The transverse momenta's associated to the "none" mode are distributed in the same way for both decay products, whereas in the other modes, lower (higher) p_t-values are favoured for e_+ (ν_e). This means that the energy of the positron (neutrino) tends to be less (more) transverse in the modes where the spin correlations are retained. When looking at the plots of the pseudorapidity, one could be surprised to see a steep drop. This is due to cuts made into the pseudorapidity of the W boson. Those were made to make sure both jets are well defined. Moreover, in the "full", "onshell" and "density" modes, the pseudorapidity of the positron is more often close to zero than in the "none" mode. This indicates that a more transverse direction of motion is favoured as the pseudorapidity goes to 0 when the particle's direction is perfectly perpendicular to the beam's axis. On the other hand, looking at η associated to ν_e, one can see that the distribution is a little bit flatter and allows more event with higher pseudorapidities in the "full","onshell" and "density" modes. This means the direction of motion is more forward towards the beam's direction. Again, spin correlation effects explain the difference that one can see between the "none" mode which does not account for spin correlation effects and the "full","onshell" and "density" modes which all retain them.

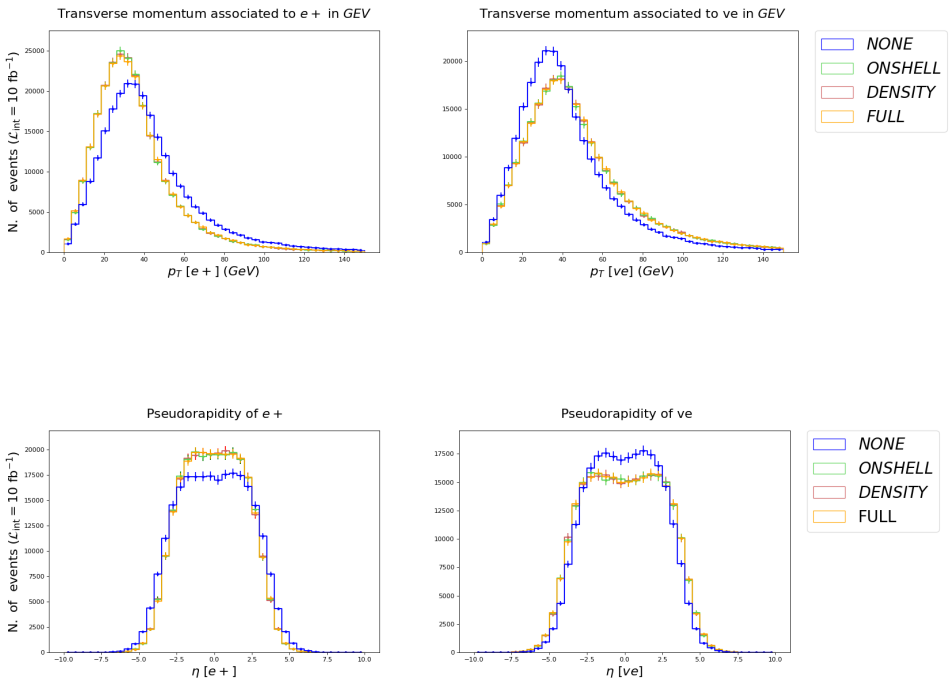

4.2.3 Decay of a colored resonance : the top quark

As stated previously, to get the final formula 45, the removal of Kroenecker delta's in favour of a simple division by the number of color was made. This was backed by an argument on the supposed SU(3) invariance of the terms considered. In the previous section, a check was made for a colorless resonance. Hence, this argument was in fact not checked at all and in order to do so, I consider the following process

$$g\ g > t\ t\sim\ ,\ \ t > w_+ b \tag{48}$$

where a top decays into a W and a b quark. The validation procedure is exactly the same as in the previous section. First, one needs to check if the ratio between methods is sufficiently close to 1. In this case, there are 48 possible helicity configurations [30] and here, since no massive particle has its mass put to zero, there are no simplifications and all 48 configurations yield non-zero matrix elements. The content of the tables is exactly the same as in the previous example and for simplicity reasons, only 5 out of the 48 helicity configurations are present in tables 6 and table 8. As in the previous example, table 6 and 8 present the matrix elements fixing the helicity for the onshell and offshell case, respectively. In tables 7 and 9, one can observe the total squared amplitude for the onshell and offshell cases.

Helicity Configuration	$\sum_{\lambda_1,\lambda_2} I^P_{\lambda_1,\lambda_2} \times I^D_{\lambda_1,\lambda_2}$	$\mathscr{M}_{s,s',r,r'}$	Ratio
[1, 1, 0, -1, -1]	3.5096640841566025	3.5096640836348376	1.000000000148665
[1, -1, 0, -1, 1]	1.1997836332771115	1.19978363310645	1.0000000001422436
[1, 1, -1, -1, -1]	0.00013982309851602235	0.00013982311505085545	0.9999998817446379
1, 1, 1, 1, -1]	5.222641115938597e-07	5.222641114037766e-07	1.0000000003639598
[1, 1, 0, -1, 1]	2.786231779925907	2.786231782178532	0.9999999991915155

Table 6: Matrix elements squared for fixed helicity in the case of the decay of an onshell top quark

g g $> t\ t\sim, t > w_+$ b	Total Matrix Element Squared	Ratio
MadGraph	23.93525063546489	1.0000000003346792
MadSpin Density	23.93525064347552	

Table 7: Total matrix element squared for both methods and their ratios for the decay of an onshell top quark

[30] Two possible helicities for the gluons, the antitop and the b, and 3 for the W, meaning $2^4 \times 3 = 48$.

Helicity Configuration	$\sum_{\lambda_1,\lambda_2} I^P_{\lambda_1,\lambda_2} \times I^D_{\lambda_1,\lambda_2}$	$\mathscr{M}_{s,s',r,r'}$	Ratio
[1, -1, 0, -1, -1]	0.22354438634018575	0.22354438601190824	1.0000000014685115
[-1, 1, 0, 1, -1]	0.00032798488887051472	0.00032798488843671777	1.0000000008184202
[-1, -1, 1, -1, 1]	0.6391942615359308	0.6391942593741528	1.0000000033820362
[-1, 1, 1, 1, -1]	6.422316319723665e-08	6.422316314467748e-08	1.0000000008183834
[1, 1, 1, -1, 1]	1.6279844309544447	1.6279844323504689	0.999999999142483

Table 8: Matrix elements squared for fixed helicity in the case of the decay of an offshell top quark

g g > t $t\sim$, t > w_+ b	Total Matrix Element Squared	Ratio
MadGraph	28.99381274830165	1.0000000006587069
MadSpin Density	28.993812767400073	

Table 9: Total matrix element squared for both methods and their ratios for the decay of an offshell top quark

As in the previous example, all methods match closely both for an onshell or an offshell resonance that, here, do possess color. Moreover, the same plots of the transverse momentum and pseudorapidity can be made using MadAnalysis5. These are shown in figure 10 to 13. In this process, all modes are equivalent, meaning that the effect of spin correlations are negligible in this case. However, the fact that the Density mode performs as well as others is a first step to convince oneself that the removal of the Kroenecker delta's in favour of a simple division by the number of possible colors of the resonance is justified. To further justify this procedure, the next subsection is dedicated to the decay of another colored particle belonging to BSM physics, the gluino.

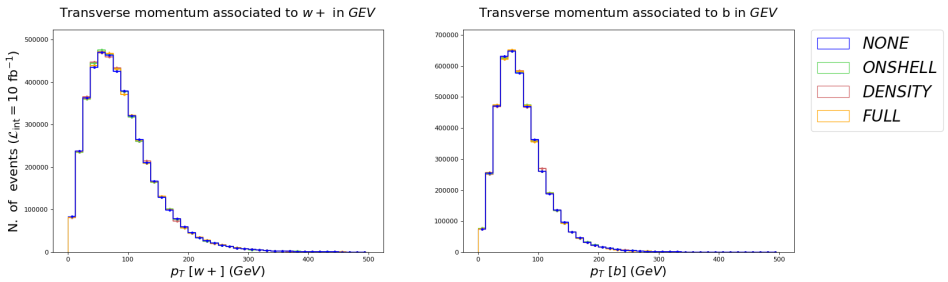

4.2.4 Decay of a SUSY particle : the gluino

As stated in the introduction, the objective of this Master's thesis is to provide tools to design a new mode within MadSpin aiming at performing decays that were currently not available in MadGraph such as loop induced processes or interferences. However, some BSM physics are already implemented in MadGraph and it can be interesting to

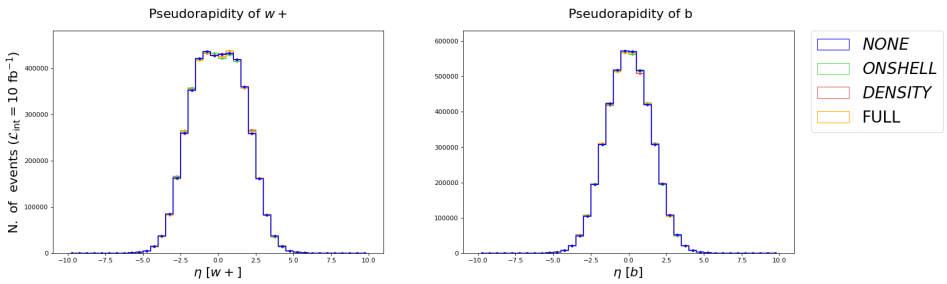

check whether formula 45 works in those cases as well. It would be even more relevant if this BSM particle had color since it would allow a furhter check of the delta's removal procedure. This is why the process considered now involves the decay of a gluino, a supersymmetric Majorana fermion, which is a color octet instead of color triplet in the case of decay of the top quark. In order to do this, the following process is considered

$$u\, u \sim > go\, go \;\;,\;\; go > uul \sim \tag{49}$$

where the gluino decays into a u quark and a left-handed anti-u. In this process there are 16 helicity configurations [31] and only 4 contribute due to the simplification of putting the mass of the quarks to zero. Here, only the case of the decay of an onshell resonance has been done and no plots were generated, as the Density mode can currently perform one decay only and in this case, there is an ambiguity between both final state gluinos. Nonetheless, the results shown in table 10 and table 11 display again very close correspondence between all methods confirming the validity of the removal procedure. One can therefore conclude that the Kroenecker delta's that encoded color conservation can indeed be replaced by a division by the number of color of the resonance. Moreover, this example highlights the fact the "density" mode can indeed treat BSM physics. In fact, as long as MadGraph is able to produce the production and decay parts for a particular process, MadSpin's density mode should always work.

4.3 Drawbacks and limitations

The previous sections were dedicated to the explanation and validation of the formula introduced in 4.1. Results were derived for colorless and colorful onshell or offshell decaying particles as well as one BSM example proving the usefulness of MadSpin's Density

[31] 2^4 since the helicity is fixed for the left-handed anti-u.

Helicity Configuration	$\sum_{\lambda_1,\lambda_2} I^P_{\lambda_1,\lambda_2} \times I^D_{\lambda_1,\lambda_2}$	$\mathscr{M}_{s,s',r,r'}$	Ratio
[-1, 1, -1, 0, 1]	0.07765322789001267	0.07765322788870756	0.9999999999831931
[-1, 1, -1, 0, -1]	0.007393292246673261	0.0073932922512833735	1.0000000006235534
[1, -1, -1, 0, 1]	0.07694651373815813	0.07694651373741054	0.9999999999902844
[1, -1, -1, 0, -1]	0.007683936280246968	0.007683936278414437	0.9999999997615114

Table 10: Matrix elements squared for fixed helicity in the case of the decay of an onshell gluino

$u\ u \sim > go\ go\ ,\ go > uul \sim$	Total Matrix Element Squared	Ratio
MadGraph	0.16967697015509103	1.000000000004272
MadSpin Density	0.1696769701558159	

Table 11: Total matrix element squared for both methods and their ratios for the decay of a gluino

mode. Nonetheless, improvements could be made if one wants to make this mode available for the general public.

As stated in the validation section, currently no offshell components are kept in MadSpin density. This is due to the fact that the offshell polarization states associated to the resonance are not available in MadSpin's standalone mode. However, as shown previously this is not a critical flaw as the order of offshell effects were shown to be quite negligible in the cases considered. This makes the implementation of those offshell terms less relevant as they would also require some hard work.

The second and more critical limitation that Madspins's density mode has, is the fact it only allows decaying one of the final state particles. This clearly is not physical as in 4.2.3 both the top and the antitop should decay. Moreover, it prevented the plots in the case of the gluino decay to be made as one could only decay one of the gluinos. This was a problem since MadSpin does not know which of the final state gluinos it should decay and thus decay both which is not possible in "density" mode currently. However, this is not a theoretical problem and equation 45 could be derived for an arbitrary number of decays. They main reason why this was not implemented is because of time constraints. There was not enough time to try to implement this feature. the other being that the sums in equation 45 become more complex and a finer analysis would have been needed. In conclusion, one can say that the possibility to allow more decays within a process would be a very nice feature to add.

5 Conclusion

Throughout this Master's thesis, the focus has been on providing tools in order to implement a new mode within MadSpin. This new mode dubbed "density", aims at providing MadSpin with matrix elements when MadGraph is not able to do so, such as in the case of loop induced processes or interferences between the Standard Model and some BSM models. The NWA, that allows this factorization between production and decay that is used throughout this work, is explained comprehensively and the proof of the validity of this approximation in the limit where $\Gamma \to 0$, made. This description is followed by an extended section on MadSpin's different available modes. Their use cases as well as their limitations are stated. On the one hand, the biggest limitation of MadSpin's none mode is the lack of spin correlation and finite width effects. On the other hand, the limitation that the "full" and "onshell" modes share is the dependence on MadGraph's capacity to produce matrix elements associated to the full event. This prevents those modes from decaying particles associated to loop-induced processes for which MadGraph cannot compute full matrix elements.

This motivates the introduction of a new mode within MadSpin dubbed "density". This mode aims at providing matrix elements using only information about production and decay while still keeping spin correlation effects. However, no finite width effects are retained within MadSpin density. In this sense, this mode is completely equivalent to the "onshell" one when Madgraph is able to compute the amplitudes associated to the full process.

The theory associated with MadSpin's density mode is described and the Master equation 45 derived. Subsequently, checks between MadSpin's different modes and "density" were made for 3 different processes to validate the procedure. One expects an equivalence between "onshell" and "density" while "offshell" and "none" should differ from them depending on the size of finite width effects and on the impact of spin correlations, respectively. Through theses 3 processes, one can observe a negligible impact of the offshell effects when looking at the transverse momentum and the pseudorapidity. This indicates that, even tough MadSpin's density mode does not include them as they are currently not retrievable in MadGraph's standalone mode, this method can be used in the case of slightly offshell resonances. On the contrary, spin correlations prove to be quite important in the case of the decay of a W boson following its production alongside two jets. There is a

statistically significant difference between the modes that do keep spin correlations and the "none" mode hinting at the importance of those in certain processes. This section also highlights the $\frac{1}{N_C}$ factor denoting the number of colors of the resonance that was introduced in the Master formula 45 to remove unpractical Kroenecker delta's. In order to convince oneself that this procedure actually works, checks were made for the decay of a color triplet, the top quark, but also for a color octet embodied by the gluino.

Those checks validate the pertinence of the Master equation 45. Nonetheless, improvements need to be made in order to make this mode available to the general public. As explained previously, when looking at the decay of a top quark and a W boson, offshell effects do not appear to be large enough to make their implementation in MadSpin's density the most relevant improvement as of now. Yet, this new method is currently not able to decay more than one of the final state particles. In addition to not being physical [32], it prevents the production of plots in the case of the gluino as there is an ambiguity between which final state gluino to decay and both cannot be decayed using "density". This is not a theoretical problem as the procedure introduced in 4.1 could be used for an arbitrary number of decays but rather a problem tied to time constraints. Still, some work is needed to treat the complex sums in 45 for more than one decay. In spite of this limitation, the Master formula 45 is fully validated and implemented within MadSpin for one decay cases and should now be usable for new cases such as loop induced processes. However, due to very technical reasons that would require some additional fixing no plots for loop-induced processes can be found in this Master's thesis.

Throughout this Master's thesis, a variety of tools and techniques needed to compute matrix elements, using only the production and decay parts of a process, were implemented. Hence, this Master's thesis constructs the architecture of MadSpin's density mode upon which additional features can be developed. The latter is left for future research.

[32] If the top decays why not the anti-top ?

References

[1] J. Alwall, R. Frederix, S. Frixione, V. Hirschi, F. Maltoni, O. Mattelaer, H. S. Shao, T. Stelzer, P. Torrielli, and M. Zaro. The automated computation of tree-level and next-to-leading order differential cross sections, and their matching to parton shower simulations. *JHEP*, 07:079, 2014.

[2] Johan Alwall, Michel Herquet, Fabio Maltoni, Olivier Mattelaer, and Tim Stelzer. MadGraph 5 : Going Beyond. *JHEP*, 06:128, 2011.

[3] Pierre Artoisenet, Rikkert Frederix, Olivier Mattelaer, and Robbert Rietkerk. Automatic spin-entangled decays of heavy resonances in Monte Carlo simulations. *JHEP*, 03:015, 2013.

[4] Diogo Buarque Franzosi, Olivier Mattelaer, Richard Ruiz, and Sujay Shil. Automated predictions from polarized matrix elements. *JHEP*, 04:082, 2020.

[5] Priscila de Aquino, William Link, Fabio Maltoni, Olivier Mattelaer, and Tim Stelzer. ALOHA: Automatic Libraries Of Helicity Amplitudes for Feynman Diagram Computations. *Comput. Phys. Commun.*, 183:2254–2263, 2012.

[6] Stefano Frixione, Eric Laenen, Patrick Motylinski, and Bryan R. Webber. Angular correlations of lepton pairs from vector boson and top quark decays in Monte Carlo simulations. *JHEP*, 04:081, 2007.

[7] Michelangelo L. Mangano. The Color Structure of Gluon Emission. *Nucl. Phys. B*, 309:461–475, 1988.

[8] H. Murayama, I. Watanabe, and Kaoru Hagiwara. HELAS: HELicity amplitude subroutines for Feynman diagram evaluations. 1 1992.

[9] C. F. Uhlemann and N. Kauer. Narrow-width approximation accuracy. *Nucl. Phys. B*, 814:195–211, 2009.

Appendix

A Gamma Properties

(i) $\gamma^{0\dagger} = \begin{pmatrix} \mathbf{1}_{2\times2} & 0 \\ 0 & -\mathbf{1}_{2\times2} \end{pmatrix}^{\dagger} = \begin{pmatrix} \mathbf{1}_{2\times2} & 0 \\ 0 & -\mathbf{1}_{2\times2} \end{pmatrix} = \gamma^0$

(ii) Since $\{\gamma^\mu\gamma^\nu\} = 2g^{\mu\nu}$, $\{\gamma^0\gamma^0\} = 2\gamma^0\gamma^0 = 2g^{00} = 2\times\mathbf{1} \longrightarrow \gamma^0\gamma^0 = \mathbf{1}$

(iii) By definition, for $k = 1,2,3$; $\gamma^{k\dagger} = \begin{pmatrix} 0 & \sigma_k \\ -\sigma_k & 0 \end{pmatrix}^{\dagger} = \begin{pmatrix} 0 & -\sigma_k \\ \sigma_k & 0 \end{pmatrix} = -\gamma^k$ and by (i), $\gamma^{0\dagger} = \gamma^0$. Thus, $\gamma^0\gamma^{0\dagger}\gamma^0 = \gamma^0$ and $\gamma^0\gamma^{k\dagger}\gamma^0 = -\gamma^0\gamma^k\gamma^0 = \gamma^k\gamma^0\gamma^0 - 2g^{0k}\gamma^0 = \gamma^k$ where we used that $\{\gamma^\mu\gamma^\nu\} = 2g^{\mu\nu}$ and $g^{0k} = 0$ for $k \neq 0$

B Factorization into production and decay

Let's go back to equation 25 and write the phase space variable explicitly

$$\sigma = \int |\mathscr{M}|^2 D(q^2)\ (2\pi)^4\delta^4\Big(P - q - \sum_{i=3}^{n} p_i\Big)\Big(\prod_{k=3}^{n}\frac{d^3\vec{p}_{d_k}}{(2\pi)^3 2E_{d_k}}\Big)\frac{d^3\vec{p}_q}{(2\pi)^3 2E_q}\times \tag{50}$$

$$\times\frac{dq^2}{2\pi}\times\delta^4\Big(q - p_{d_1} - p_{d_2}\Big)\frac{d^3\vec{p}_{d_1}}{(2\pi)^3 2E_{d_1}}\frac{d^3\vec{p}_{d_2}}{(2\pi)^3 2E_{d_2}}.$$

In the limit $\Gamma \to 0$ the denominator D simplifies

$$= \int |\mathscr{M}|^2\frac{\delta(q^2 - M^2)}{2\Gamma M}\ (2\pi)^4\delta^4\Big(P - q - \sum_{i=3}^{n} p_i\Big)\Big(\prod_{k=3}^{n}\frac{d^3\vec{p}_{d_k}}{(2\pi)^3 2E_{d_k}}\Big)\frac{d^3\vec{p}_q}{(2\pi)^3 2E_q}\times \tag{51}$$

$$\times\frac{dq^2}{2\pi}\times\delta^4\Big(q - p_{d_1} - p_{d_2}\Big)\frac{d^3\vec{p}_{d_1}}{(2\pi)^3 2E_{d_1}}\frac{d^3\vec{p}_{d_2}}{(2\pi)^3 2E_{d_2}}.$$

The integration over q^2 can be performed using the Dirac delta

$$= (2\pi)^4\int\frac{\delta^4\Big(P - q - \sum_{i=3}^{n} p_i\Big)}{2\Gamma M}\ \Big(\prod_{k=3}^{n}\frac{d^3\vec{p}_{d_k}}{(2\pi)^3 2E_{d_k}}\Big)\frac{d^3\vec{p}_q}{(2\pi)^3 2E_q}\times \tag{52}$$

$$\times\frac{dq^2}{2\pi}\times\delta^4\Big(q - p_{d_1} - p_{d_2}\Big)\frac{d^3\vec{p}_{d_1}}{(2\pi)^3 2E_{d_1}}\frac{d^3\vec{p}_{d_2}}{(2\pi)^3 2E_{d_2}}|\mathscr{M}|^2\Big|_{q^2=M^2}.$$

Performing the same procedure using $\mathscr{M}_{NWA}$ and subtracting both results, one gets

$$\sigma_{full} - \sigma_{NWA} = (2\pi)^4 \int \frac{\delta^4\left(P - q - \sum_{i=3}^{n} p_i\right)}{2\Gamma M} \left(\prod_{k=3}^{n} \frac{d^3\vec{p}_{d_k}}{(2\pi)^3 2E_{d_k}}\right) \frac{d^3\vec{p}_q}{(2\pi)^3 2E_q} \frac{dq^2}{2\pi} \times \quad (53)$$

$$\times \delta^4\left(q - p_{d_1} - p_{d_2}\right) \times \frac{d^3\vec{p}_{d_1}}{(2\pi)^3 2E_{d_1}} \frac{d^3\vec{p}_{d_2}}{(2\pi)^3 2E_{d_2}} \left[|\mathscr{M}_{full}|^2 - |\mathscr{M}_{NWA}|^2\right]\Big|_{q^2=M^2} \quad .$$

Clearly, since all the terms on the second line are Lorentz's invariant, the whole line is invariant under Lorentz's transformations. This allows to choose a reference frame in which the decaying particle is at rest, i.e. $q = (E_q, \vec{0})^T$. Or under the NWA assumption, one can write $q = (M, \vec{0})^T$. Integrating out $\vec{p_{d_2}}$, writing only the bottom line in the previous equation and going into spherical coordinates for the remaining integral $dp_{d_1} = p_{d_1}^2 dp_{d_1} d\Omega_{d_1}$ yields

$$\int \frac{p_{d_1}^2 dp_{d_1}}{2E_{d_1}} \delta\left(E_p - E_{d_1} - E_{d_2}\right) \times \int d\Omega_{d_1} \left[|\mathscr{M}_{full}|^2 - |\mathscr{M}_{NWA}|^2\right]\Big|_{\vec{p}_{d_1}=-\vec{p}_{d_2}, E_q=M}. \quad (54)$$

$\mathscr{M}_p^\mu$ and $\mathscr{M}_d^\nu$ are not Lorentz invariant but Lorentz 4-vectors. Thus, one can conclude that $\mathscr{M}_p^\mu$ must depend on $p_{d_3}, ..., p_{d_n}$ and $\mathscr{M}_d^\nu$ on p_{d_1} and p_{d_2} since there are no other possible Lorentz 4-vectors in production or decay, respectively. Looking at equation 54, all momenta's are fixed expect p_{d_1}. Hence, $\mathscr{M}_p^\mu$ is fixed and $\mathscr{M}_d^\nu$ depends on p_{d_1}. The choice of solid angle is therefore $d\Omega_{d_1} = d\Phi_{d_1} dcos(\theta_{d_1})$ where θ_{d_1} is the angle between $\vec{\mathscr{M}}_p$ and $\vec{p}_{d_1}$, and where $\mathscr{M}_p^\mu = (\mathscr{M}_p^0, \vec{\mathscr{M}}_p)^T$. Restricting the problem to the case of a bosonic decaying particle [33] for which, in the reference frame chosen, $P_{\mu\nu} = -g_{\mu\nu} + \frac{q_\mu q_\nu}{M^2} = diag(0, \mathbf{1}_3)$, the full matrix elements and the NWA one can be written as

$$|\mathscr{M}_{full}|^2 = |\vec{\mathscr{M}}_p \cdot \vec{\mathscr{M}}_d|^2 = |\mathscr{M}_p|^2 |\mathscr{M}_d|^2 cos(\theta_1)^2 \quad , \quad |\mathscr{M}_{NWA}|^2 = \frac{1}{3} |\mathscr{M}_p|^2 |\mathscr{M}_d|^2. \quad (55)$$

The integration over θ_{d_1} can now be performed

$$|\mathscr{M}_p|^2 |\mathscr{M}_d|^2 \int_{-1}^{1} d\theta_{d_1} \left(cos(\theta_{d_1})^2 - \frac{1}{3}\right) = 0. \quad (56)$$

This proves that computing the matrix element in the NWA limit by factorizing production and decay as in 29 does not introduce errors for an onshell decaying particle.

[33] The fermionic case follows the same procedure with the following propagator $P_{\mu\nu} = \not{q} + M$

C Phase Space Points

C.1 W boson decay following production of $W_+ jj$

- Onshell case. The two first two quarks are the initial state particles and the two last are the decay products :

Onshell	E	p_x	p_y	p_z
u	2.0845630727E+03	+0.0000000000	+0.0000000000	+2.0845630727E+03
u	5.50497995143+02	-0.0000000000	-0.0000000000	-5.5049799514E+02
w_+	2.0028571650E+03	-1.0561192364E+01	+2.7899679707E+00	+2.0012122038E+03
u	5.4817603918E+02	+1.6760255225E+00	-2.5408454310E+01	-5.4758430521E+02
d	8.4027863668E+01	+8.8851668411E+00	+2.2618486340E+01	+8.0437178957E+01
u	1.8314128699E+03	+9.2711896647E+00	+1.4630064031E+01	+1.8313309658E+03
$d\sim$	1.7144428059E+02	-1.9832381952E+01	-1.1840096081E+01	+1.6988122350E+02

- Offshell case :

Offshell	E	p_x	p_y	p_z
u	+2.78404166470E+02	0.00000000000	0.00000000000	+2.78404166470E+02
u	1.72941042920*E+03	0.00000000000	0.00000000000	-1.72941042920*E+03
w_+	4.366441546030E+02	-1.292607722940E+01	-1.456257539850E+02	-4.027294881830E+02
u	2.911458891370E+02	+1.698726652880E+02	+8.500661929170E+01	+2.206424279830E+02
d	1.280024551930E+03	-1.569465880590E+02	+6.06191346930E+01	-1.268919202530E+02
u	1.316771578040E+02	+3.377772574230E+01	-5.104721430960E+01	-1.165852522510E+02
$d\sim$	3.049669967990E+02	-4.670380297170E+01	-9.45785396750E+01	-2.861442359330E+02

C.2 Decay of a colored resonance : the top quark

- Onshell case :

Onshell	E	p_x	p_y	p_z
g	2.3618981955E+03	+0.0000000000	+0.0000000000	+2.3618981955E+03
g	1.3970308806E+01	-0.0000000000	-0.0000000000	-1.3970308806E+01
t	1.2333326893E+03	-2.5240334839E+00	+5.4879247747E+01	+1.2199026272E+03
$t\sim$	1.1425358150E+03	+2.5240334839E+00	-5.4879247747E+01	+1.1280252595E+03
W_+	7.9999929202E+03	-2.0995426144E+01	+1.0006321018E+02	+7.8935302453E+02
b	4.3333339587E+02	+1.8471392663E+01	-4.5183962497E+01	+4.3054960128E+02

- Offshell case :

Offshell	E	p_x	p_y	p_z
g	2.1935380990E+01	+0.0000000000	+0.0000000000	+2.1935380990E+01
g	1.8788891478E+03	-0.0000000000	-0.0000000000	-1.8788891478E+03
t	1.0268867956E+03	+9.7534849534E+01	+3.8632913630E+01	-1.0067581348E+03
$t\sim$	8.7393773322E+02	-9.7534849534E+01	-3.8632913630E+01	-8.5019563199E+02
W_+	5.3260466521E+02	+1.3714325887E+01	+7.4685715903E+01	-5.2099373754E+02
b	4.9428212863E+02	+8.3820523480E+01	-3.6052802339E+01	-4.8576439553E+02

C.3 Decay of a SUSY particle : the gluino

The onshell phase space point used is :

Onshell	E	p_x	p_y	p_z
u	2.0575289177E+03	+0.0000000000	+0.0000000000	2.0575289177E+03
$u\sim$	3.7850198915E+02	-0.0000000000	-0.0000000000	3.7850198915E+02
go	1.1513359974E+03	+6.2602404174E+02	-1.1244460871E+02	+7.4277099225*E+02
go	1.2846949094E+03	-6.2602404174E+02	+1.1244460871E+02	+9.3625593631E+02
u	1.4215430357E+02	+6.9395025445E+01	-2.6725115985E+01	+1.2115256763E+02
$ul\sim$	1.0091816939E+03	+5.5662901634E+02	-8.5719492732*E+01	+6.2161842467E+02